Veterinary Microbiology 232 (2019) 13–21

Contents lists available at ScienceDirect

Veterinary Microbiology

journal homepage: www.elsevier.com/locate/vetmic

Characterization and epidemiological survey of porcine sapelovirus in China

Ying Li[a,d,1], Liuyang Du[a,d,1], Tao Jin[c], Yao Cheng[a,d], Xin Zhang[e], Shaoyong Jiao[a,d], Tong Huang[a,d], Yu Zhang[a,d], Yan Yan[b], Jinyan Gu[a,b,d,*], Jiyong Zhou[b]

[a] MOE Joint International Research Laboratory of Animal Health and Food Safety, Institute of Immunology, Nanjing Agricultural University, Nanjing 210095, China
[b] Key Laboratory of Animal Virology of Ministry of Agriculture, Department of Veterinary Medicine, Zhejiang University, Hangzhou 310058, China
[c] China National Genebank-Shenzhen, BGI-Shenzhen, Shenzhen, 518083, China
[d] Jiangsu Engineering Laboratory of Animal Immunology, College of Veterinary Medicine, Nanjing Agricultural University, Nanjing 210095, China
[e] Division of Swine Infectious Diseases, State Key Laboratory of Veterinary Biotechnology, Harbin Veterinary Research Institute of the Chinese Academy of Agriculture Sciences, Harbin 150069, China

ARTICLE INFO

Keywords:
Porcine sapelovirus (PSV)
Biological characterization
Pathogenic
High prevalence

ABSTRACT

Porcine sapelovirus (PSV) is a causative agent of acute diarrhoea, respiratory distress, reproductive failure, and polioencephalomyelitis in swine. Here, we report the isolation, genomic sequence, and biological characterization of PSV isolated from pig diarrhoeal samples. In our study, two PSV strains were identified with a diameter of approximately 25 nm, and their full genomes were 7564 nucleotides in length. We named the strains PSV-JXXY-a2 and PSV-JXXY-c. Phylogenetic analysis showed that the two virus isolates were classified into the China cluster. Moreover, the PSV-JXXY-a2 strain could be inactivated quickly at 54℃ and adapted to grow on different cell lines of porcine, human, and baby hamster origin. Pathogenicity investigation showed that the isolated PSV could infect neonatal piglets efficiently and caused diarrhoea in piglets. Further epidemiological investigation revealed a high prevalence of PSV in pig herds, and the PSV-positive rates in pigs with diarrhoea were much higher than in asymptomatic samples in China. Together, our findings demonstrate that PSV-JXXY-a2 is pathogenic to neonatal piglets and advance knowledge on the prevalence of PSV infection.

1. Introduction

Porcine sapelovirus (PSV) is a non-enveloped, positive-sense single-stranded genomic RNA virus that was previously designated porcine enterovirus 8 in the genus *Enterovirus* and is now classified into the genus *Sapelovirus* in the family *Picornaviridae* (Tseng and Tsai, 2007). To date, the genus *Sapelovirus* consists of porcine sapelovirus, simian sapelovirus, avian sapelovirus and unclassified sapelovirus, including bat, California sea lion, marmot, mouse and WUHARV sapelovirus. The genome of PSV is approximately 7.5 kb and has a genomic organization similar to that of other picornaviruses: a 5′ untranslated region (UTR), a large open reading frame (ORF), a 3′ UTR and a poly (A) tail (Racaniello, 2001). The large ORF encodes a single polyprotein that is subsequently cleaved into four structural proteins (VP4, VP2, VP3 and VP1) and seven functional proteins (2A, 2B, 2C, 3A, 3B, 3C and 3D) (Lan et al., 2011; Oberste et al., 2002).

PSV is an important pathogen worldwide (Abe et al., 2011; Bak et al., 2017; Buitrago et al., 2010; Prodelalova, 2012); it has been reported to be associated with acute diarrhoea, respiratory distress, reproductive failure, and polioencephalomyelitis in swine and mainly transmits by a faecal-oral route, although PSV infection in swine is most frequently asymptomatic (Abe et al., 2011; Lamont and Betts, 1960; Lan et al., 2011; Schock et al., 2014). One study from Korea revealed that there were no differences in the PSV infection rate between diarrhoea and non-diarrhoea specimens (Bak et al., 2017), but another viral metagenomics analysis in faecal samples demonstrated that PSV was more prevalent in diarrhoeic pigs than in healthy pigs (Zhang et al., 2014). Notably, a recent report demonstrated that the Korean PSV strain SV-A is enteropathogenic in piglets, producing significant lesions in the intestines, and severe villous atrophy associated with high viral RNA loads (Kim et al., 2016).

Here, we describe the isolation of PSV from swine diarrhoeic faecal samples and molecular and biological characterization of PSV isolates. Moreover, molecular and serological investigation revealed that PSV was highly prevalent in Chinese pigs.

* Corresponding author at: MOE Joint International Research Laboratory of Animal Health and Food Safety, Institute of Immunology, Nanjing Agricultural University, Nanjing 210095, China.
E-mail address: gjy@njau.edu.c (J. Gu).
[1] Two authors are equal to this work.

https://doi.org/10.1016/j.vetmic.2019.02.017
Received 22 September 2018; Received in revised form 6 February 2019; Accepted 10 February 2019

2. Materials and methods

2.1. Cells

Swine testicular (ST) cells (kindly provided by professor Yaowei Huang, Zhejiang University, China), porcine kidney (PK-15) cells (CCL-33; ATCC), intestinal porcine enterocytes (IPEC-J2) (C0668; Shanghai Guandao Biotechnology Co., Ltd., China), baby hamster kidney (BHK-21) cells (CCL-10; ATCC), human embryonic kidney (293 T) cells (CRL-11268; ATCC), adenocarcinomic human alveolar basal epithelial cells A549 (CCL-185; ATCC), Madin-Darby canine kidney (MDCK) cells (CCL-34; ATCC) and chicken fibroblast (DF-1) cells (CRL-1746; ATCC) were maintained in our laboratory. ST, BHK-21, 293 T, A549, MDCK and DF-1 cells were cultured at 37 °C in 5% CO_2 in Dulbecco's modified Eagle's medium (DMEM; Gibco). PK-15 cells were cultured at 37 °C in 5% CO_2 in minimum essential medium (MEM; HyClone). IPEC-J2 cells were cultured at 37 °C in 5% CO_2 in RPMI-1640 medium (Gibco). All media were supplemented with 10% foetal bovine serum (FBS; Biological Industries).

2.2. Virus isolation

Ten diarrhoeic faecal specimens were collected from 3-day-old diarrhoeic piglets from four different farms of Xinyu city, Jiangxi Province, in 2016. Three specimens, JXXY-a1, -a2, and -a3, were from farm A; three specimens, JXXY-b1, -b2, and -b3, were from farm B; three specimens, JXXY-F3, -F4, and -F5, were from farm C; and one specimen, JXXY-c, was from farm D. Virus isolation was performed on these ten diarrhoeic faecal specimens using ST cells. Briefly, samples were diluted 10-fold with DMEM containing antibiotics (penicillin and streptomycin), vortexed for 30 s and centrifuged at 3500 × g for 10 min. Then, the supernatants were filtered through 0.22 μm pore membrane filters (Merck Millipore Ltd. United States). Filtered supernatants were used to inoculate confluent monolayers of ST cells at 37 °C and 5% CO_2 and observed daily for 3 days to monitor the development of cytopathic effects (CPEs). At 3 days post-infection (dpi), the culture supernatants were collected and passaged on ST cells 4 times. The viral isolates were purified by plaque assay.

2.3. RNA extraction, deep sequencing and assembly

Viral RNA was extracted from the plaque-purified viruses using a QIAamp Viral RNA Mini Kit (QIAGEN, Germany) and subjected to next-generation sequencing on an Illumina MiSeq platform (Huada Gene Technology Co. Ltd.). Viral RNA was qualified by an Agilent Technologies 2100 Bioanalyzer. Reverse transcription polymerase chain reaction (RT-PCR) was conducted using Superscript II reverse transcriptase (Invitrogen) with the random primers N6. Paired-end libraries with insert sizes of 130–170 base pairs were subsequently constructed using a standard protocol provided by BGI (BGI-Shenzhen) and then sequenced on the BGISEQ-500 platform in PE100 mode (Goodwin et al., 2016).

Raw data were obtained and filtered by SOAPnuke [options: -l 10 -q 0.1 -n 0.01] (v.1.5.6; https://github.com/BGI-flexlab/SOAPnuke). The high-quality reads were processed to remove host contaminant reads by using SOAP (Li et al., 2009) based on the reference genome of *Sus scrofa* (GenBank assembly accession: GCA_000003025.6). The non-host reads were mapped to the virus database using SOAP to screen the candidate viruses (with the number of mapped reads ≥100). The non-host reads were de novo assembled using IDBA-UD (Peng et al., 2012) with the default options. We also used MAQ (Li et al., 2008) to perform reference-based assembly with the genome of PSV and improved the results from IDBA-UD. Finally, apart from the 5′ and 3′ UTR sequences, the main segments of the PSV genome were obtained and identified using BLAST (Altschul et al., 1990) against the NCBI nucleotide (nt) database.

To obtain the complete genomes of the two isolated PSV strains, primer pairs were designed to amplify 5′ and 3′ UTR sequences based on the Korean PSV strain KS04105 (GenBank accession no. KJ821019, Supplemental Table S1). PCR products were individually purified and cloned using the Mighty TA-cloning Kit (TaKaRa Bio Inc.) followed by Sanger sequencing to determine the sequences. The genomes were assembled and analysed using the DNASTAR program.

2.4. Preparation of anti-PSV antibody

Antiserum produced by pigs was acquired as approved by the Institutional Animal Care and Ethics Committee of Nanjing Agricultural University (permit no. IACECNAU2016102). Six 1-day-old conventional pigs were divided into two groups (n = 3) and housed in two separate enclosures. Piglets in group 1 were immunized thrice (ten days apart) intramuscularly with 1.5 mL inactivated PSV antigens mixed with adjuvant. The inactivated virus was prepared by incubating 6 parts formalin (Sigma) with 94 parts PSV-JXXY-a2 supernatant ($10^{6.94}$ PFU/mL) at room temperature for 12 h and then homogenized with Freund's complete adjuvant (Sigma), a well-known adjuvant with water-in-oil emulsion. Piglets in group 2 were used as negative controls. Piglets were terminated by intravenously receiving Euthol solution two weeks after the final immunization, and serum was collected from each piglet and stored at -80°C.

2.5. Immunofluorescence assay (IFA)

To examine the capability of PSV to infect various cells, ST, PK-15, IPEC-J2, BHK-21, 293 T, A549, MDCK and DF-1 cells were inoculated with PSV-JXXY-a2 at a multiplicity of infection (MOI) of 0.5. The inoculated ST, PK-15, BHK-21 and 293 T cells were cultured for 10 h, and the inoculated IPEC-J2, A549, MDCK and DF-1 cells were cultured for 48 h. After incubation, the cells were fixed with 4% paraformaldehyde, incubated with anti-PSV sera (diluted 1:100) for 1 h at 37°C, and then incubated with a FITC-conjugated-secondary antibody (KPL) for 1 h at 37°C. Cellular nuclei were stained with 10 μg/mL DAPI (Roche) for 5 min, and samples were examined by fluorescence microscopy (ECLIPSE Ti-S, Nikon, Japan).

2.6. In vitro growth characterization and temperature sensitivity

The virus titres of PSV-JXXY-a2 for each time point were determined by plaque assay in ST cells with modifications, as described previously (Hu et al., 2015). Briefly, after the overlay-covered cells were incubated at 37°C for 60 h, the plates were fixed and stained with 1% (w/v) crystal violet in 20% EtOH and 5% formaldehyde for at least 2 h. Then, the plaques were counted, and the virus titres were expressed as PFU/mL. To further examine the temperature sensitivity of PSV, PSV-JXXY-a2 was heated at 37, 42, 50, 51, 52, 53, 54, and 55°C for the indicated time, and then virus titres (TCID50/mL) were determined in triplicate in ST cells by IFA.

2.7. Virus purification and electron microscopy

ST cell monolayers were infected with PSV-JXXY-a2 at an MOI of 0.5 for 48 h. The cells were subjected to three freeze-thaw cycles. The cellular debris was clarified by centrifugation at 4807 × *g* at 4 °C for 15 min. Crude virus was pelleted from the clarified supernatant by ultracentrifugation at 92,600 × *g* at 4 °C for 3 h. The virus pellet was resuspended in 0.4 mL DMEM and was then layered onto a 20–60% (w/v) discontinuous iodixanol solution (OptiPrep™ Density Gradient Medium, Sigma-Aldrich) by centrifugation at 126,100 × *g* at 4 °C for 2.5 h. The virus band at the interface was collected and detected by Hitachi Model H-7650 transmission electron microscopy (TEM).

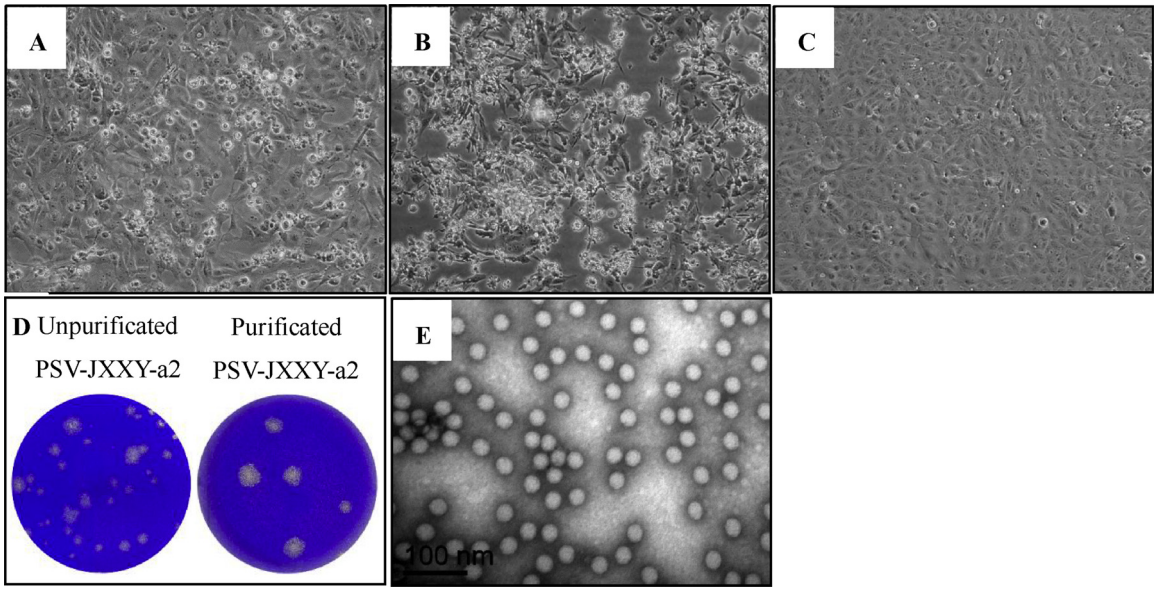

Fig. 1. Isolation and identification of PSV. CPE, plaque purification and electron microscopy of PSV-JXXY-a2 in ST cells. (A) ST cells infected with PSV-JXXY-a2 strain showed shrinking, rounding and lifting morphology at 15–18 hpi. (B) Infected ST cell monolayers were completely detached at 24–36 hpi. (C) Mock-infected ST cells. (D) Plaques of unpurified and purified PSV-JXXY-a2 strain. (E) Electron microscopy of purified PSV-JXXY-a2 virions.

2.8. Sequence and phylogenetic analysis

Nucleotide sequences and deduced amino acid (aa) sequences of the polyprotein gene and individual genes of PSV isolates were compared with those of other known picornaviruses (Supplemental Table S2) using multiple alignments conducted with the Clustal W program. Phylogenetic analyses were performed based on nucleotide sequences by the neighbour-joining method in MEGA 7.0. Bootstrap values were calculated with 1000 replicates. Structural homology modelling of the PSV VP1 protein was performed by the SWISS-MODEL server (https://www.swissmodel.expasy.org/).

2.9. Animal experiments

Ethics approval of animal experiments was as described for the antiserum produced in pigs. Neonatal healthy conventional piglets, RNA negative for PSV, Porcine epidemic diarrhea virus (PEDV), Porcine deltacoronavirus (PDCoV), Transmissible Gastroenteritis Virus (TGEV), genogroup A rotavirus (GARV), and mammalian orthoreovirus (MRV) in the faecal samples, selected from one sow that was PSV, PEDV, and PDCoV RNA and antibody negative, were housed in a HEPA-filtered level 2 biosecurity facility. Piglets were fed a milk-replacement diet (Anyou, China) instead of colostrum and breast milk. Four one-day-old neonatal piglets were divided into two groups. Piglets in group 1 (V1-V2) were each challenged orally with 5 mL PSV-JXXY-a2 ($10^{6.94}$ PFU/mL, $10^{8.20}$ copies/mL); piglets in group 2 (C1–C2) received 5 mL DMEM orally as negative controls. All piglets were monitored daily for rectal temperature and clinical signs, and a faecal consistency score was assigned to each piglet using a subjective scale wherein 0 is normal, 1 is pasty, 2 is creamy and 3 is watery. Piglets with faecal consistency scores of 2 or 3 were scored as diarrhoea positive. Faecal swabs were collected from all piglets for viral RNA detection were at 0, 1, 2, 3, and 4 dpi. All piglets received Euthol solution intravenously to be euthanized at 5 dpi. The heart, liver, spleen, lung, kidney, tonsil, cerebellum, cerebrum, spinal cord, submaxillary nodes, inguinal lymph nodes, bladder and alimentary tract were collected from each piglet for viral RNA detection, and the alimentary tract was sampled separately from the stomach, duodenum, jejunum, ileum, caecum, colon, rectum and mesenteric lymph nodes. Virus shedding from faeces or tissues was tested by qRT-PCR as described previously. The intestinal contents collected from V1 and V2 piglets were used for virus re-isolation on ST cells.

2.10. Epidemiological investigation

For the molecular epidemiological survey of PSV, a total of 185 clinical samples, including faeces, faecal swabs and intestine, were collected between February 2016 and March 2017 from sows, finishers and nursing piglets that were asymptomatic or with clinical diarrhoea in different commercial pig herds in the provinces of Anhui, Fujian, Jiangxi, Guangxi, Zhejiang, Jiangsu, Hubei, Hunan, Shandong, Liaoning and Shanghai in China (Fig. 6A). All samples were investigated for PSV and porcine epidemic diarrhoea virus (PEDV). PSV detection was performed using qRT-PCR screening for the 5′ untranslated region as previously reported by Chen et al. (Chen et al., 2014). The method used for detecting PEDV was as previously reported (Song et al., 2006).

For the serological epidemiological survey, 258 pig serum samples were collected between February and December 2017 from commercial pig herds in Gansu, Shanxi, Hebei, Beijing, Shandong, Jiangsu, Anhui, Zhejiang, Fujian, Jiangxi, Hunan, Hubei, Guangxi and Hainan provinces in China (Fig. 6C). The PSV-specific antibody titres were determined by IFA as previously described. Briefly, ST cells were inoculated with PSV at an MOI of 1 for 12 h, and then IFA was performed using the 258 serum samples with 4-fold serial dilutions. All samples were tested in triplicate.

2.11. Statistical analysis

Summary statistics were calculated to assess the overall quality of the data. All data were processed using GraphPad Prism software (version 7.0). *In vitro* experiments were carried out independently at least 3 times, and the *t*-test was used to evaluate the statistical significance of the virus titres. Statistical significance was set to a *P*-value of 0.05.

3. Results

3.1. Isolation and identification of PSV strains

ST cells were inoculated with ten diarrhoeic faecal specimens that were PDCoV RNA positive but PEDV, TGEV, GARV and MRV RNA

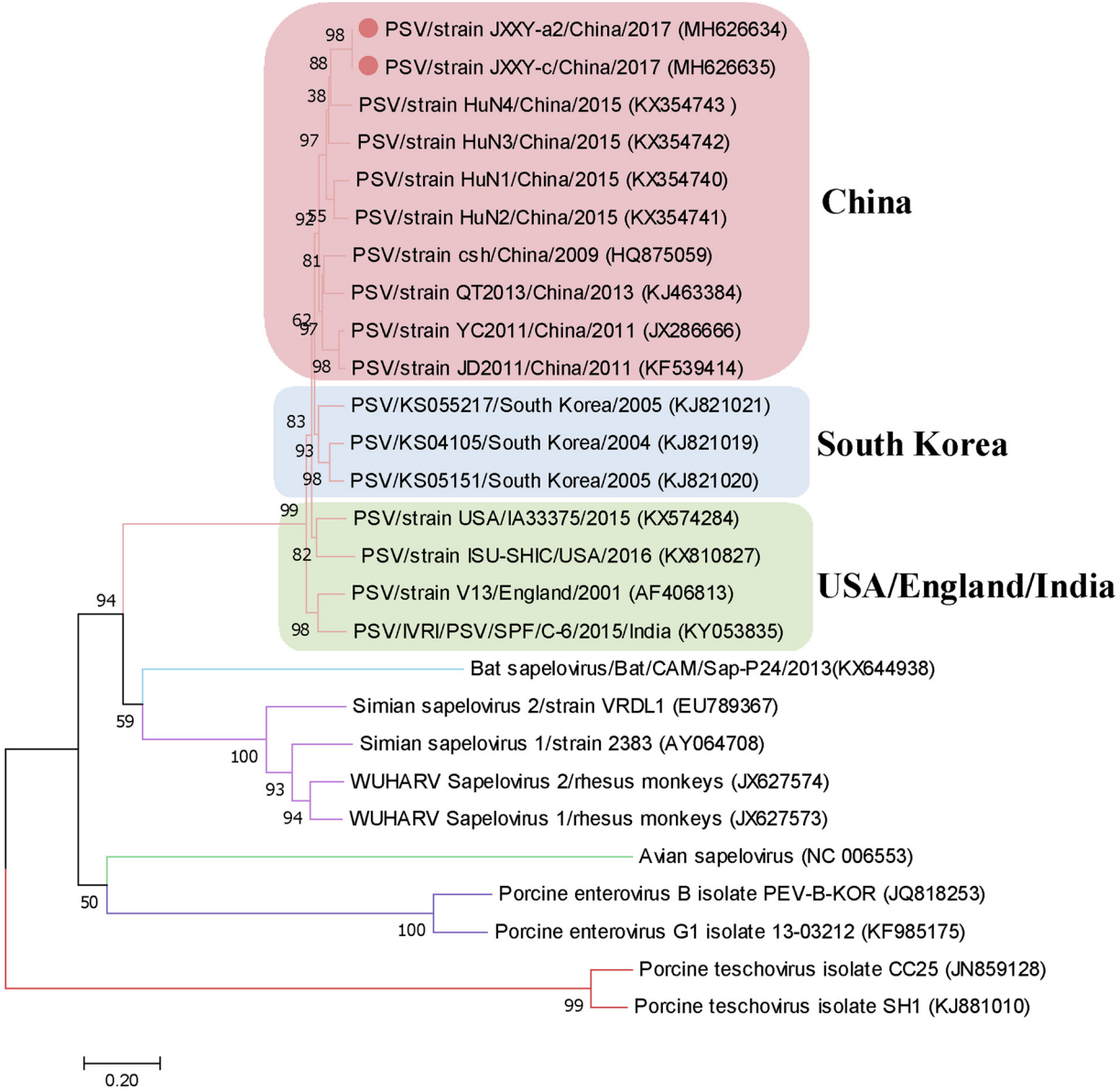

Fig. 2. Phylogenetic analysis of the polyprotein nucleotide sequence for PSV-JXXY-a2 and PSV- JXXY-c strains. A phylogenetic tree was constructed using the neighbour-joining method with 1000 bootstrap replicates. The branch length is indicated at each branch node.

negative. After 2 blind passages in ST cell monolayers, two samples, JXXY-a2 and JXXY-c, showed CPEs with shrinking, rounding and lifting morphology after 48–52 hpi. Unexpectedly, RNA extracted from these two isolates was negative for PDCoV. After 4 serial passages, ST cells inoculated with these two isolates showed visible CPEs after 15–18 hpi, and infected cell monolayers were completely detached by 24–36 hpi in comparison with mock-infected cells (Fig. 1A–C). Plaque assays showed that the plaques were approximately 3.5 mm in diameter after three purifications (Fig. 1D). TEM observations revealed icosahedral, non-enveloped viral particles with a diameter of approximately 25 nm (Fig. 1E). Next-generation sequencing revealed these two isolates to be PSV, and no other viral matches were detected. These results confirm that these two virus isolates are PSVs, and they are named PSV-JXXY-a2 and PSV-JXXY-c (GenBank accession no. MH626634 and MH626635).

3.2. Full genome sequence and phylogenetic analyses

The two isolates, PSV-JXXY-a2 and PSV-JXXY-c, have the same genomic organization, excluding the poly(A) tail. The length of the complete genomes is 7564 nt, including a 489 nt 5′ UTR sequence, a 6996 nt polyprotein gene and a 79 nt 3′ UTR sequence. As shown in Supplemental Table 2, the length of the complete genomes of PSV-JXXY-a2/c is different from all of the other reference PSV strains. The length of the polyprotein gene is varied in PSV strains and ranges from 6969 nt to 6999 nt; however, it is relatively conserved in Chinese PSVs with a 6996 nt length, except for the HuN4 strain with a three-nucleotide insertion. According to a previous study, the 5′ terminal nucleotide residues of PSV should be UU (Son et al., 2014); PSV-JXXY-a2/c are consistent with these sequence features, but in the reference strains, only KS04105, KS05151, KS055217 and IA33375 have the complete 5′ UTR sequences; and between these sequences, the length of the 5′ UTR ranges from 489 nt to 491 nt. The complete 3′ UTR sequences have been widely reported, and the length is relatively conserved, commonly being 79 nt and 82 nt.

The encoding regions of the PSV genome, including the polyprotein gene, capsid-coding region (P1 gene) and genes of mature peptides cleaved from P1 protein (VP1, VP2 and VP3), were phylogenetically analysed (Fig. 2). The phylogenetic tree of the polyprotein gene showed

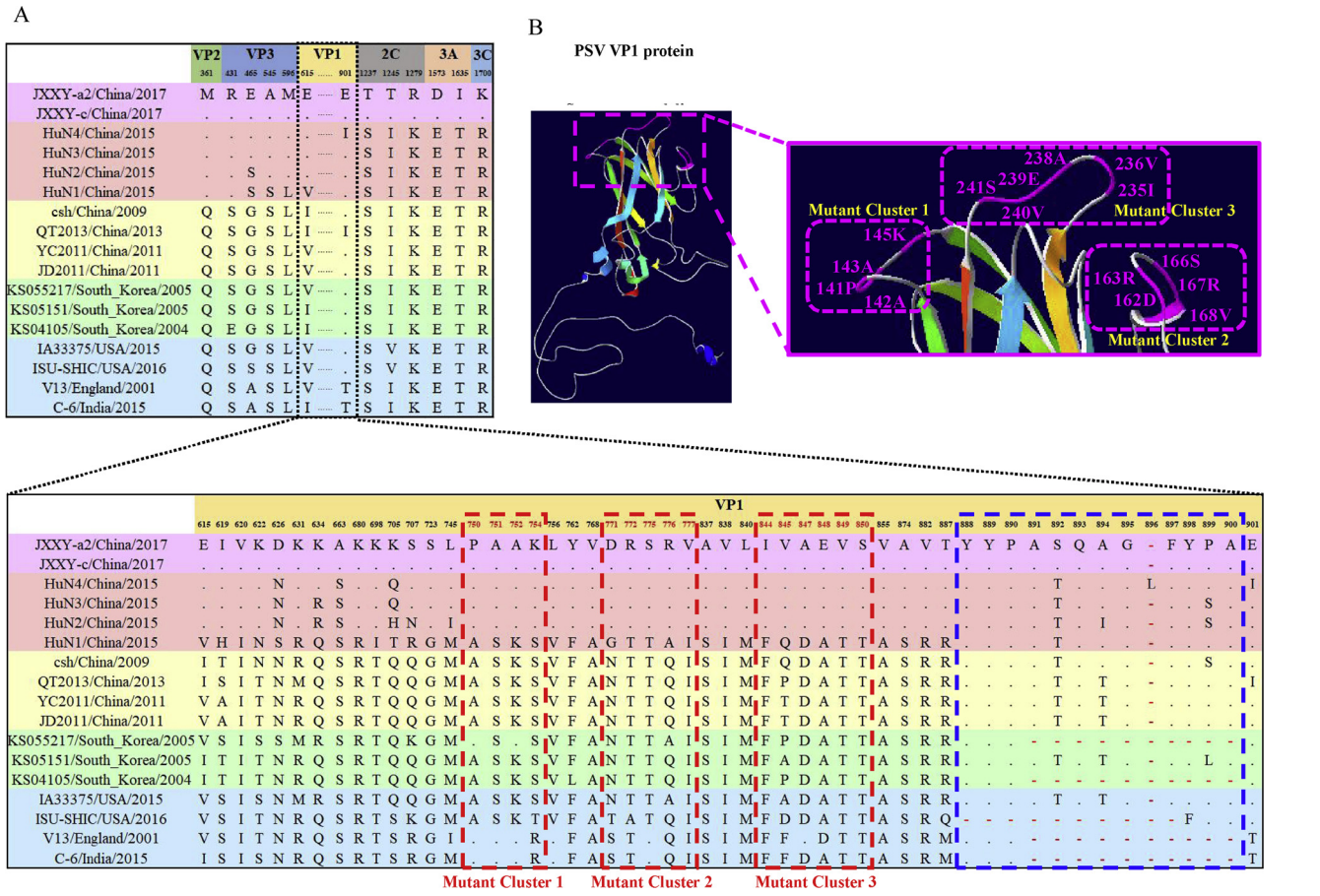

Fig. 3. Analysis of the deduced amino acid sequences of PSV polyprotein. (A) The differences in deduced amino acids in the polyproteins of the isolated PSV and reference strains. The dots represent amino acid residues that are identical to the PSV-JXXY-a2 strain. Boxes with red dashed lines indicate three mutant clusters in VP1 protein. Boxes with blue dashed lines indicate the varied region in the 3′ end of VP1 protein, and the red bars indicate the precise positions of deletions. (B) Illustration of the predicted three-dimensional structure of the PSV-JXXY-a2 VP1 protein. The protein modelling of the PSV VP1 protein monomer was built using SWISS-MODEL, and the mutant amino acids mapped to the three mutant clusters are boxed with rose dashed lines. (For interpretation of the references to colour in this figure legend, the reader is referred to the web version of this article).

that the genus *sapelovirus* is more closely related to *Enterovirus* than to *Teschovirus*. In the *sapelovirus* genus, porcine sapelovirus is most closely related to Bat sapelovirus. The PSV isolates, along with 25 complete polyprotein sequences of picornavirus strains available in the NCBI database, showed that all of the PSV strains are classified into three distinct clusters correlated with their geographical location, China, South Korea and USA/England/India. PSV-JXXY-a2 and PSV-JXXY-c are classified into the China cluster, which is more closely related to the South Korea PSV cluster.

3.3. Comparative analysis of the deduced amino acid sequence of the polyprotein

To investigate the genetic relationships and characteristics between PSVs and the genetics of PSV-JXXY-a2 and PSV-JXXY-c, sequence alignments of the deduced amino acids of the polyprotein were compared with the representative reference PSV strains from different clusters in the polyprotein gene phylogenetic tree. The data revealed that the deduced amino acid sequences of PSV-JXXY-a2 and PSV-JXXY-c polyproteins were identical, and they shared many molecular similarities with Chinese HuN2/3/4 strains. Compared with other reference strains, PSV-JXXY-a2/c had amino acid substitutions in all of the twelve mature peptides (L-VP4-VP2-VP3-VP1-2A-2B-2C-3A-3B-3C^{pro}-3D^{pro}) cleaved from polyprotein, and the significant substitutions in VP2, VP3, VP1, 2C, 3A and 3C are shown in Fig. 3A. Among these mature peptides, VP1 was the most hypervariable protein, with three mutant clusters and a varied 3′ end sequence. Mutant cluster 1, including four adjacent amino acid mutations, was located at positions 750–752 and 754. Mutant cluster 2, including five amino acid mutations, was located at positions 771, 772 and 775 − 777. Mutant cluster 3, including six amino acid mutations, was located at positions 844, 845, and 847 − 850. Structural homology-modelling of PSV VP1 monomer protein with the template of human enterovirus 71 VP1 protein (3zfe.1.A in the SWISS-MODEL template library) revealed that these three mutant clusters of VP1 protein were located in three loops that are probably exposed on the virion surface (Fig. 3B). In addition, the varied 3′ end sequence of the VP1 protein was located at position 888 − 900. It is interesting that the different lengths of polyproteins mainly resulted from this 3′ end-varied region. With the same 3′ end sequence, strains of JXXY-a2/c, HuN1/2/3, QT2013, YC2011, JD2022, csh, KS05151, and IA33375 have the same length as VP1 protein (2332 aa). HuN4 has a one amino acid longer VP1 protein (2333 aa) due to a single amino acid insertion at position (896 L) in the 3′ end sequence. KS055217/KS04105 (2324 aa) and V13/C-6 (2323 aa) have shorter VP1 proteins because of a nine-amino-acid deletion at position (891ASQAGF-YPA900); another nine-amino-acid deletion at position (888YYPASQ-AGF897) led to the shorter VP1 protein (2324 aa) of the ISU-SHIC strain (Fig. 3A).

Excluding three mutant clusters and the varied 3′ end sequence of the VP1 protein, another significant amino acid substitution existed in the polyprotein. Ten amino acid residues, 626D, 663A, 705 K, 892S, 1237 T, 1245 T, 1279R, 1573D, 1635I and 1700 K, were identical only

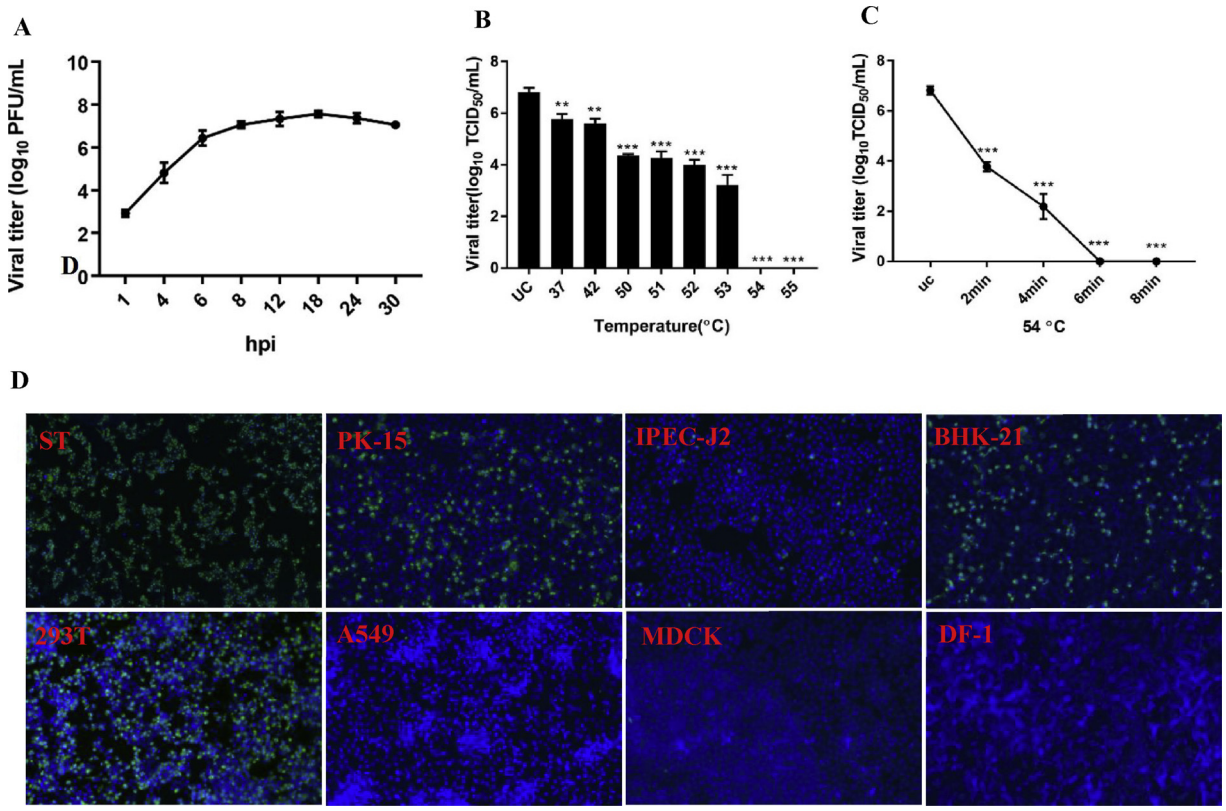

Fig. 4. Growth kinetics, temperature sensitivity and cellular adaptation of PSV-JXXY-a2. (A) *In vitro* growth kinetics curve of PSV-JXXY-a2. ST cell monolayers were infected with PSV-JXXY-a2 at an MOI of 0.5 and were harvested at 1, 4, 6, 8, 12, 18, 24 and 30 hpi. Virus titres (PFU/mL) were determined in ST cells in triplicate using plaque assays. (B) Temperature sensitivity of PSV-JXXY-a2. Virus titres ($TCID_{50}$/mL) were determined in triplicate after treatment at 37, 42, 50, 51, 52, 53, 54℃ and 55℃ for 1 h. The unheated PSV (UC) was used as a positive control. (C) Minimum time for inactivating PSV-JXXY-a2 at the most effective temperature. Virus titres ($TCID_{50}$/mL) were determined in triplicate after treatment at 54℃ for 2, 4, 6 and 8 min. Experiments of growth kinetics and temperature sensitivity were carried out independently at least 3 times, and the mean values of the log-transformed titres are shown ± the standard error of the mean (SEM). Differences in the titres were evaluated by a two-tailed *t*-test with the threshold of statistical significance indicated (** $P < 0.01$; *** $P < 0.001$). (D) Infectivity of PSV-JXXY-a2 in different cell species was determined by IFA using anti-PSV serum. All cell lines were infected with PSV-JXXY-a2 at an MOI of 0.5. ST, PK-15, BHK-21 and 293T cells were fixed at 10 hpi. IPEC-J2, A549, MDCK and DF-1 cells were fixed at 48 hpi.

in PSV-JXXY-a2/c strains. Twenty amino acid residues at positions 545A, 596 M, 615E, 619I, 620 V, 622 K, 631 K, 680 K, 698 K, 723 K, 756 L, 762Y, 768 V, 837A, 838 V, 840 L, 855 V, 874A, 882 V and 887 T were identical between PSV-JXXY-a2/c and HuN2/3/4 but different from other reference strains (Fig. 3A).

3.4. Temperature sensitivity and cellular adaptation of the PSV isolate

To detect the virus growth kinetics, ST cells were inoculated with PSV-JXXY-a2 at an MOI of 0.5 for the indicated time points. The virus titre presented a gradual upward tendency and reached the highest peak ($10^{7.57}$ PFU/mL) at 18 hpi (Fig. 4A), revealing that the PSV-JXXY-a2 strain could infect and replicate efficiently in ST cells. To detect temperature sensitivity, PSV strain JXXY-a2 was heated at the indicated temperatures for 1 h and then used to inoculate ST cell monolayers. Compared with the untreated control, the JXXY-a2 infectivity decreased significantly after exposure to 37℃ for 1 h, and with a continuous increase in treatment temperature, the virus titre continued to decrease (Fig. 4B). JXXY-a2 retained infectivity at 53℃ for 1 h but was inactivated completely at 54℃ for only 6 min (Fig. 4C). These results revealed that 54℃ is the most effective temperature to inactivate PSV. To assess cell adaptation to different cell lines, the infection ability of PSV strain JXXY-a2 was examined with various cell lines, including ST, PK-15, IPEC-J2, BHK-21, 293 T, A549, MDCK and DF-1 cells. As shown in Fig. 4D, JXXY-a2 could not only infect ST, PK-15 and IPEC-J2 but also infect BHK-21 and 293 T very efficiently. However, A549 and MDCK were not susceptible to PSV infection. Our results indicate that the PSV-JXXY-a2 strain has broad cell tropism *in vitro*.

3.5. PSV is pathogenic to neonatal piglets

To determine whether the isolated PSV-JXXY-a2 strain is an enteric pathogen in pigs, two one-day-old, neonatal, healthy conventional piglets were inoculated with PSV-JXXY-a2. No significant temperature changes or obvious clinical signs were observed at 1, 2 and 3 dpi in any of the four piglets. At 4 dpi, two PSV-inoculated piglets developed watery diarrhoea (score of 3) compared to two mock-inoculated piglets (Fig. 5A–B). Due to the severe clinical signs of diarrhoea in two of the PSV-inoculated piglets, all piglets were terminated at 5 dpi. To further explore the virus shedding and the viral antigen distribution in PSV orally inoculated piglets, daily faecal swabs and tissue samples derived from all piglets were collected for viral RNA detection. Faecal virus shedding showed that high levels of viral RNAs were shed in faecal samples of PSV-infected pigs at 2–4 dpi (Fig. 5C). Furthermore, viral RNAs could be detected in all of the alimentary tract organs, and the levels of viral RNAs were higher in the cecum, colon and rectum than in the duodenum, jejunum, ileum, stomach and mesenteric lymph nodes (Fig. 5D). Moreover, a higher level of PSV RNA was detected in the tonsil, inguinal lymph nodes and bladder than in the spleen, lung, cerebellum, cerebrum and submaxillary nodes, but viral RNAs were not detected in the heart, liver, kidney and spinal cord (Fig. 5E). Furthermore, the virus re-isolation from PSV-infected intestinal contents showed obvious CPE at 42 hpi, and a large number of PSV-positive cells were observed in IFA with the antiserum specific for PSV (Fig. 5A).

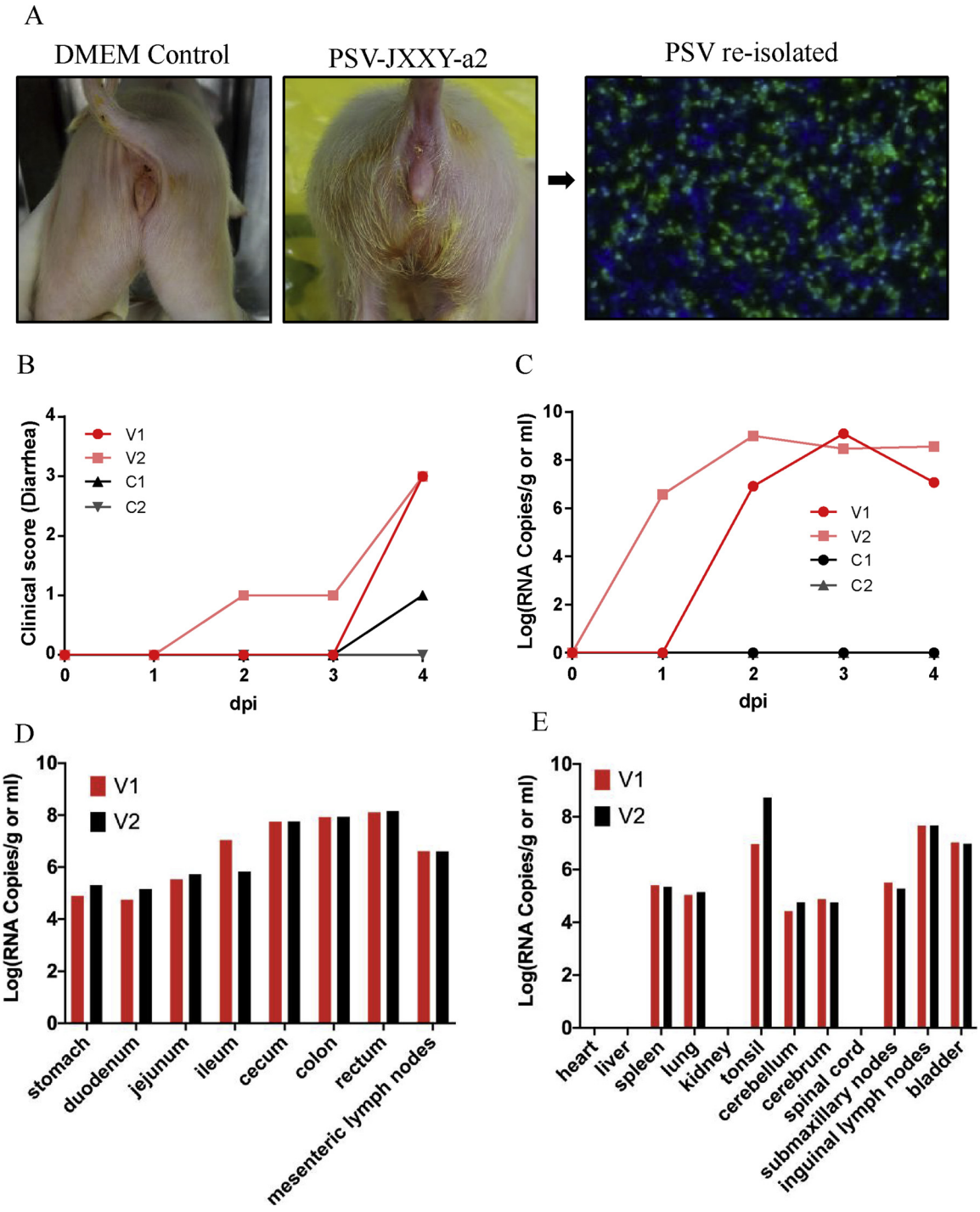

Fig. 5. Pathogenicity of the PSV-JXXY-a2 strain in neonatal piglets. (A) Clinical signs in PSV-JXXY-a2- and mock-infected neonatal piglets. Representative PSV-infected neonatal piglets (V1 and V2) showing clinical signs of diarrhoea, piglets (C1 and C2) inoculated with DMEM showing no obvious clinical signs. ST cells inoculated with filtered intestinal contents collected from PSV-JXXY-a2-infected piglets for 42 h showed a large number of PSV-positive cells by IFA. (B) Faecal consistency scores in PSV-JXXY-a2- and mock-infected neonatal piglets. PSV-inoculated piglets (V1 and V2) developed watery diarrhoea (score of 3) compared to DMEM-inoculated piglets (C1 and C2), the clinical score of diarrhoea: 1 is pasty, 2 is creamy, and 3 is watery. (C) Viral RNA shedding in faecal swabs after virus and DMEM inoculation. High levels of viral RNAs were shed in faecal samples of PSV-infected pigs (V1 and V2) at 2–4 dpi, and faecal swabs from DMEM-inoculated piglets (C1 and C2) were PSV viral RNA-negative. (D–E) Viral RNA distribution in the alimentary tract and tissues from PSV-inoculated piglets (V1 and V2). (D) Viral RNAs were detected in all of the alimentary tract organs, and the levels of viral RNAs were higher in the caecum, colon and rectum than in the duodenum, jejunum, ileum, stomach and mesenteric lymph nodes. (E) Higher levels of PSV RNAs were detected in the tonsil, inguinal lymph nodes and bladder than in the spleen, lung, cerebellum, cerebrum and submaxillary nodes; however, viral RNAs were not detected in the heart, liver, kidney and spinal cord.

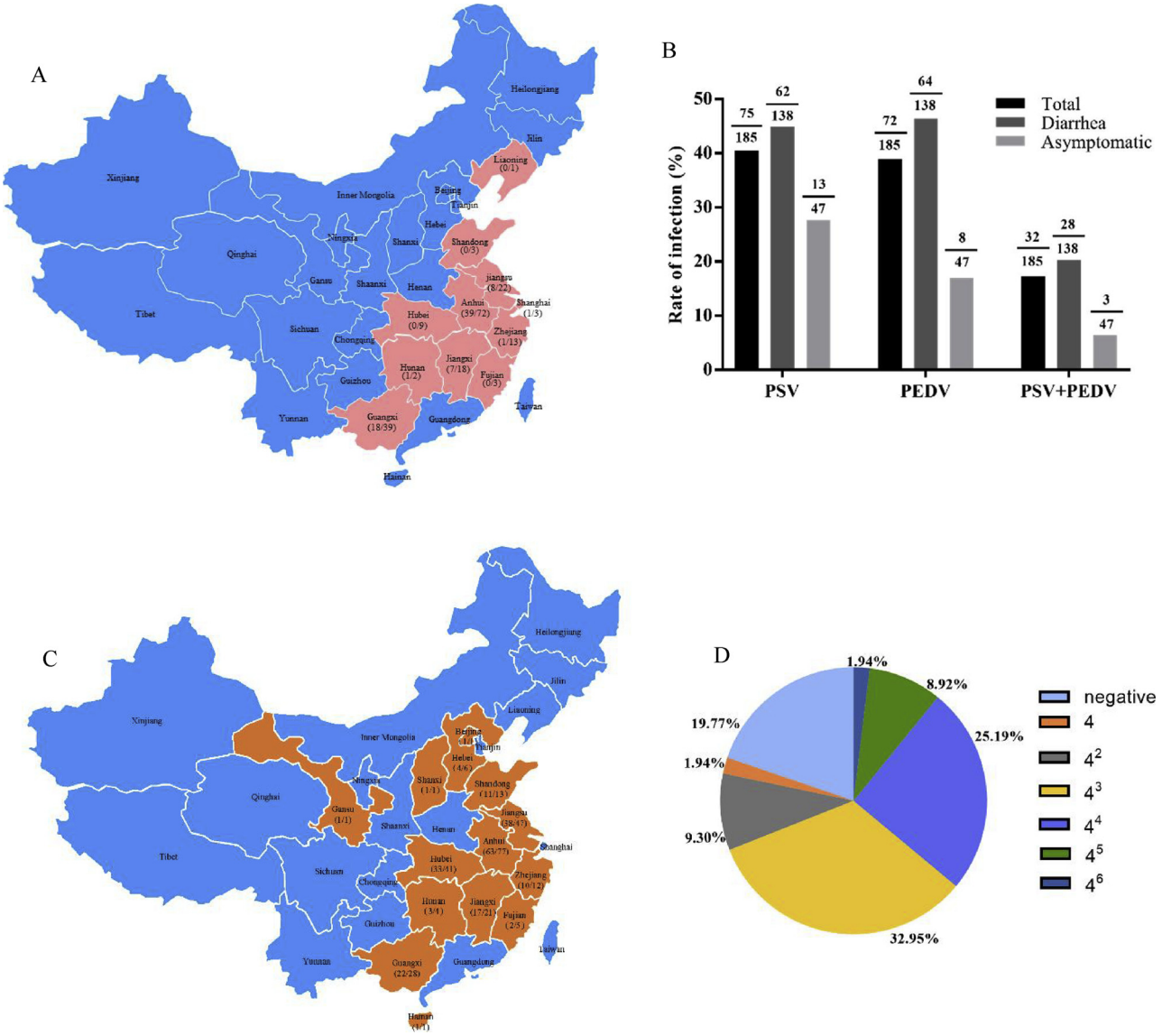

Fig. 6. Epidemiological investigation of PSV infection. (A–B) Viral investigation of PSV infection. (A) Pink colour represents provinces sampled for PSV investigation. The numbers in brackets indicate PSV-positive/total samples. (B) Rates of positive PSV, PEDV and PSV-PEDV co-infection in diarrhoea, asymptomatic and total collected samples. (C–D) Serological investigation of PSV infection. (C) Orange colour represents provinces sampled for PSV serological investigation. The numbers in brackets represent the ratios of PSV serum-positive/total serum samples. (D) Sero-prevalence and antibody titres of PSV determined by IFA. (For interpretation of the references to colour in this figure legend, the reader is referred to the web version of this article).

These data demonstrate that PSV-JXXY-a2 is pathogenic to piglets.

3.6. Epidemiological investigation of PSV infection in pig herds

To evaluate the frequency of PSV infection, a total of 185 samples (138 with clinical diarrhoea and 47 asymptomatic) were collected and investigated by qRT-PCR. As shown in Fig. 6B, of the 185 samples, 75 were PSV positive (40.54%), 72 were PEDV positive (39.92%), and 32 were PSV/PEDV double positive (17.30%). Notably, all of the positive rates of PSV (44.93%, 62/138), PEDV (46.38%, 64/138) and co-infection of PSV/PEDV (20.29%, 28/138) in diarrhoea samples were much higher than in asymptomatic samples, which were 27.66% (13/47), 17.02% (8/47) and 6.38% (3/47), respectively. Meanwhile, for sero-epidemiological investigation, a total of 258 pig serum samples were collected and investigated by IFA. As shown in Fig. 6D, a high PSV positive rate (80.23%, 207/258) was observed in collected sera. Additionally, 68.99% (178/258) of the total samples had a titre greater than 4^3, over half had a titre between 4^3 and 4^4, and 10.85% (18/258) had a titre greater than 4^5. Collectively, these results revealed that PSV infection was highly prevalent in pig herds and that the proportion of PSV infection in diarrhoea samples was higher than in asymptomatic samples.

4. Discussion

In summary, we isolated, sequenced and genetically characterized two PSV strains, PSV-JXXY-a2 and PSV-JXXY-c, from diarrhoeal samples in pig farms of Jiangxi Province in 2016 and demonstrated pathogenicity in neonatal piglets.

The PSV capsid protein VP1 is the most external viral protein, which contains a number of major neutralization sites (Mateu, 1995). The VP1 protein is considered to be immunodominant and has proved to be valuable in determining genetic relationships among picornaviruses (Oberste et al., 1999; Son et al., 2014). A homology comparison of the deduced VP1 amino acid sequences in this study revealed that PSV-JXXY-a2, PSV-JXXY-c and Chinese HuN strains have three mutant

clusters compared with other reference strains. Structural homology modelling found that these three mutant clusters are located on the surface loops of the VP1 protein. Loops exposed on the virion surface are the most variable regions of picornavirus virions and are considered to be the most important neutralizing immunogenic sites (Plevka et al., 2012; Rossmann et al., 1985; Sherry et al., 1986). Thus, whether these three mutant clusters are responsible for the neutralizing immunogenicity needs to be further investigated. Additionally, the C-terminus of VP1 can induce neutralizing antibodies in many picornaviruses (Foo et al., 2007; Mateu, 1995); therefore, it is worth noting if the varied 3′ end sequence of PSV VP1 protein is associated with neutralizing antigenic sites.

Due to the near identical nucleotide and deduced amino acid sequences of PSV-JXXY-a2 and PSV-JXXY-c, the *in vitro* growth characterization, temperature-sensitivity assays, and the *in vivo* pathogenic experiments of PSV were all carried out with the representative strain PSV-JXXY-a2. A previous study reported that PSV infection was limited to cells of porcine origin (Kim et al., 2016). Another study revealed that the human cell lines PLC/PRF/5, HepG2/C3a and the green monkey cell lines Vero E6 and PGMKC are also susceptible to PSV infection (Bai et al., 2018). Our study showed that in addition to the porcine cell lines ST, PK-15, and IPEC-J2, the human 293 T cell line and the baby hamster BHK-21 cell line are both susceptible to PSV infection. In summary, the infection of human, green monkey and baby hamster cells with PSV raises concerns about its potential host range beyond swine. However, the human cell line A549, dog cell line MDCK and chicken fibroblast cell line DF-1 were resistant to PSV in our study, and the susceptibility differences to PSV should be useful for studying receptors of PSV. Although PSV is widely distributed, it can be inactivated easily by heating at 65 °C for 5 min or 60 °C for 10 min (Bai et al., 2018); our result indicates that the minimum condition to inactivate PSV-JXXY-a2 is heating at 54 °C for 6 min, which may be due to the different PSV strains.

To date, the pathogenicity of PSV has been poorly studied, and only one PSV strain, Korean SV-A, has been well characterized for intestinal pathogenicity; it can induce diarrhoea and intestinal pathology in piglets (Kim et al., 2016). In the present study, the diarrhoeic faecal-origin PSV strain PSV-JXXY-a2 was found to replicate efficiently in the intestine and induce diarrhoea in piglets, implying that this PSV-JXXY-a2 strain may be pathogenic. Notably, epidemiological investigation in this study revealed that the PSV-positive rates and co-infection of PSV/PEDV in diarrhoea samples were much higher than in asymptomatic samples, indicating that PSV may contribute collectively to enteric disease of pigs along with other porcine pathogens; therefore, PSV cannot be ignored when controlling the diarrhoea of pigs.

Acknowledgment

This work was supported by the National Key Research and Development Program of China (Grant numbers 2017YFD0500101 and 2016YFD0500102), the Fundamental Research Funds for the Central Universities (Grant number 2017FZA6019) and the Priority Academic Program Development of Jiangsu Higher Education Institutions.

Appendix A. Supplementary data

Supplementary material related to this article can be found, in the online version, at doi:https://doi.org/10.1016/j.vetmic.2019.02.017.

References

Abe, M., Ito, N., Sakai, K., Kaku, Y., Oba, M., Nishimura, M., Kurane, I., Saijo, M., Morikawa, S., Sugiyama, M., Mizutani, T., 2011. A novel sapelovirus-like virus isolation from wild boar. Virus Genes 43, 243–248.

Altschul, S.F., Gish, W., Miller, W., Myers, E.W., Lipman, D.J., 1990. Basic local alignment search tool. J. Mol. Biol. 215, 403–410.

Bai, H., Liu, J., Fang, L., Kataoka, M., Takeda, N., Wakita, T., Li, T.C., 2018. Characterization of porcine sapelovirus isolated from Japanese swine with PLC/PRF/5 cells. Transbound. Emerg. Dis. 65, 727–734.

Bak, G.Y., Kang, M.I., Son, K.Y., Park, J.G., Kim, D.S., Seo, J.Y., Kim, J.Y., Alfajaro, M.M., Soliman, M., Baek, Y.B., Cho, E.H., Kwon, J., Choi, J.S., Park, S.I., Cho, K.O., 2017. Occurrence and molecular characterization of Sapelovirus A in diarrhea and non-diarrhea feces of different age group pigs in one Korean pig farm. J. Vet. Med. Sci. 78, 1911–1914.

Buitrago, D., Cano-Gomez, C., Aguero, M., Fernandez-Pacheco, P., Gomez-Tejedor, C., Jimenez-Clavero, M.A., 2010. A survey of porcine picornaviruses and adenoviruses in fecal samples in Spain. J. Vet. Diagn. Invest. 22, 763–766.

Chen, J., Chen, F., Zhou, Q., Li, W., Chen, Y., Song, Y., Zhang, X., Xue, C., Bi, Y., Cao, Y., 2014. Development of a minor groove binder assay for real-time PCR detection of porcine Sapelovirus. J. Virol. Methods 198, 69–74.

Foo, D.G., Alonso, S., Phoon, M.C., Ramachandran, N.P., Chow, V.T., Poh, C.L., 2007. Identification of neutralizing linear epitopes from the VP1 capsid protein of Enterovirus 71 using synthetic peptides. Virus Res. 125, 61–68.

Goodwin, S., McPherson, J.D., McCombie, W.R., 2016. Coming of age: ten years of next-generation sequencing technologies. Nat. Rev. Genet. 17, 333–351.

Hu, H., Jung, K., Vlasova, A.N., Chepngeno, J., Lu, Z., Wang, Q., Saif, L.J., 2015. Isolation and characterization of porcine deltacoronavirus from pigs with diarrhea in the United States. J. Clin. Microbiol. 53, 1537–1548.

Kim, D.S., Kang, M.I., Son, K.Y., Bak, G.Y., Park, J.G., Hosmillo, M., Seo, J.Y., Kim, J.Y., Alfajaro, M.M., Soliman, M., Baek, Y.B., Cho, E.H., Lee, J.H., Kwon, J., Choi, J.S., Goodfellow, I., Cho, K.O., 2016. Pathogenesis of Korean Sapelovirus A in piglets and chicks. J. Gen. Virol. 97, 2566–2574.

Lamont, P.H., Betts, A.O., 1960. Studies on enteroviruses of the pig IV. The isolation in tissue culture of a possible enteric cytopathogenic swine orphan (ECSO) virus (V13) from the faeces of a pig. Res. Vet. Sci.

Lan, D., Ji, W., Yang, S., Cui, L., Yang, Z., Yuan, C., Hua, X., 2011. Isolation and characterization of the first Chinese porcine sapelovirus strain. Arch. Virol. 156, 1567–1574.

Li, H., Ruan, J., Durbin, R., 2008. Mapping short DNA sequencing reads and calling variants using mapping quality scores. Genome Res. 18, 1851–1858.

Li, R., Yu, C., Li, Y., Lam, T.W., Yiu, S.M., Kristiansen, K., Wang, J., 2009. SOAP2: an improved ultrafast tool for short read alignment. Bioinformatics 25, 1966–1967.

Mateu, M.G., 1995. Antibody recognition of picornaviruses and escape from neutralization: a structural view. Virus Res. 38, 1–24.

Oberste, M.S., Maher, K., Kilpatrick, D.R., Pallansch, M.A., 1999. Molecular evolution of the human enteroviruses: correlation of serotype with VP1 sequence and application to picornavirus classification. J. Virol. 73, 1941–1948.

Oberste, M.S., Maher, K., Pallansch, M.A., 2002. Molecular phylogeny and proposed classification of the simian picornaviruses. J. Virol. 76, 1244–1251.

Peng, Y., Leung, H.C., Yiu, S.M., Chin, F.Y., 2012. IDBA-UD: a de novo assembler for single-cell and metagenomic sequencing data with highly uneven depth. Bioinformatics 28, 1420–1428.

Plevka, P., Perera, R., Cardosa, J., Kuhn, R.J., Rossmann, M.G., 2012. Crystal structure of human enterovirus 71. Science (New York, N.Y.) 336, 1274.

Prodelalova, J., 2012. The survey of porcine teschoviruses, sapeloviruses and enteroviruses B infecting domestic pigs and wild boars in the Czech Republic between 2005 and 2011. Infect. Genet. Evol. 12, 1447–1451.

Racaniello, V., 2001. Picornaviridae: The Viruses and Their Replication. Fields Virology.

Rossmann, M.G., Arnold, E., Erickson, J.W., Frankenberger, E.A., Griffith, J.P., Hecht, H.J., Johnson, J.E., Kamer, G., Luo, M., Mosser, A.G., et al., 1985. Structure of a human common cold virus and functional relationship to other picornaviruses. Nature 317, 145–153.

Schock, A., Gurrala, R., Fuller, H., Foyle, L., Dauber, M., Martelli, F., Scholes, S., Roberts, L., Steinbach, F., Dastjerdi, A., 2014. Investigation into an outbreak of encephalomyelitis caused by a neuroinvasive porcine sapelovirus in the United Kingdom. Vet. Microbiol. 172, 381–389.

Sherry, B., Mosser, A.G., Colonno, R.J., Rueckert, R.R., 1986. Use of monoclonal antibodies to identify four neutralization immunogens on a common cold picornavirus, human rhinovirus 14. J. Virol. 57, 246–257.

Son, K.Y., Kim, D.S., Kwon, J., Choi, J.S., Kang, M.I., Belsham, G.J., Cho, K.O., 2014. Full-length genomic analysis of Korean porcine Sapelovirus strains. PLoS One 9, e107860.

Song, D.S., Kang, B.K., Oh, J.S., Ha, G.W., Yang, J.S., Moon, H.J., Jang, Y.S., Park, B.K., 2006. Multiplex reverse transcription-PCR for rapid differential detection of porcine epidemic diarrhea virus, transmissible gastroenteritis virus, and porcine group A rotavirus. J. Vet. Diagn. Invest. 18, 278–281.

Tseng, C.H., Tsai, H.J., 2007. Sequence analysis of a duck picornavirus isolate indicates that it together with porcine enterovirus type 8 and simian picornavirus type 2 should be assigned to a new picornavirus genus. Virus Res. 129, 104–114.

Zhang, B., Tang, C., Yue, H., Ren, Y., Song, Z., 2014. Viral metagenomics analysis demonstrates the diversity of viral flora in piglet diarrhoeic faeces in China. J. Gen. Virol. 95, 1603–1611.